Compact ultrafast laser pulse shaping using chirped volume Bragg gratings

Filipe Ruão Marques Teixeira
filipe.ruao@tecnico.ul.pt

Instituto Superior Técnico, Lisboa, Portugal

April 2016

Abstract

The shaping of ultrafast pulses is an area of great interest in the world of laser technology, due to the multiple possibilities and applications enabled by user-defined shaped pulses. Despite the success of the several existing techniques for pulse shaping, common problems still exist, such as the large dimensions of the associated experimental setups or the sensitivity of the alignment to mechanical vibrations, which limit their use in environments outside the laboratory, such as in industrial equipment. In this work we study the feasibility of a novel alternative to the optical element that performs the spatial dispersion inside a conventional pulse modulator. Our approach consists in using a chirped volume Bragg grating, and the goal is to study the properties of the transverse spatial chirp created when a laser pulse enters on the CVBG at a given angle. We developed a simplified theoretical model that allows the calculation of the diffraction efficiency at a given depth inside the CVBG and the associated spatial chirp. Using the model, the performance was studied for several parameters of the diffraction grating and of the incident pulse. We performed a number of laboratory measurements using different experimental setups for characterizing the performance of a specific CVBG operating at 1034 nm. We compare those with the theoretical model and determine of the influence of each parameter. Finally, we analyze and discuss the future possibilities and limitations for the use of CVBG ultra-short pulse shaping.
Keywords: Ultrafast Optics, Pulse Shaping, Chirped Volume Bragg Gratings, Spatial Dispersion.

1. Introduction

Lasers are the central building block for generating ultrashort light pulses. Just two decades had passed after its invention and the duration of the shortest pulse has already decreased six orders of magnitude, coming from the nanosecond range to the femtosecond one. As we speak, 10 fs or even shorter pulses can be generated directly from compact and reliable laser oscillators and the temporal resolution of measurements has overcome the resolution of modern sampling oscilloscopes by orders of magnitude.

One key feature of such pulses is the way one can process, or shape, them. *Pulse Shaping* consists in the generation of arbitrary optical waveforms, and has been an active field of research for the last 25 years. The reason behind the recent increasing interest in this field is related to the fact that ultrafast optical pulse shaping shows significant relevance in many other areas of science and engineering. Its applications include coherent control [1–3], multidimensional spectroscopy [4], biological imaging [5], compression of optical pulses [6], factorization of numbers [7, 8] and optical communications [9]. Interested readers may find more extensive review on some of these in [10, 11].

This work's main goal is to acquire knowledge on Chirped Volume Bragg Gratings (CVBGs), and apply it in an ultrafast pulse shaping technique. CVBGs are bulked chirp Bragg gratings, in this case representing chirped mirrors, which modus operandi works with the fact that the Bragg wavelength is not constant, but varies within the structure. Thinking of an ultrashort pulse as being composed of groups of quasi-monochromatic waves, that is of a set of much longer wave packets of narrow spectrum all added together coherently, the idea is to disperse all this wavelengths in order to manipulate them in an one-by-one fashion, shaping the pulse. These gratings are known for their robustness, making them easy to align and significantly resistant to shocks and vibrations. They are also potentially suitable to reduce the size of pulse shaping systems. [12]

In order to make use of the above mentioned advantages, the objective is, then, to study the behaviour of these gratings in all their pulse shaping relevant features, mainly the dispersive ones, making possible its future integration in pulse shaping systems.

2. Fundamentals

2.1. Pulse Shaping

One way to realize a pulse shaper is the Fourier transform pulse shaper. Its operation principle is based on optical Fourier transformations from the time domain into the frequency domain and vice versa. In figure 1 a standard design of such a pulse shaper is shown. This is called the 4f design.

The incoming ultrashort laser pulse is dispersed by a grating and the spectral components are focused by a lens of focal length f. In the back focal plane of this lens - the Fourier plane - the spectral components of the original pulse are separated from each other having minimum beam waists. Thus, the spectral components can be modulated individually by placing a linear mask, $\tilde{M}(\omega)$, into the Fourier plane. Afterwards, the laser pulse is reconstructed by performing an inverse Fourier transformation back into the time domain. Optically, this is realized by a mirrored setup consisting of an identical lens and grating [10, 13].

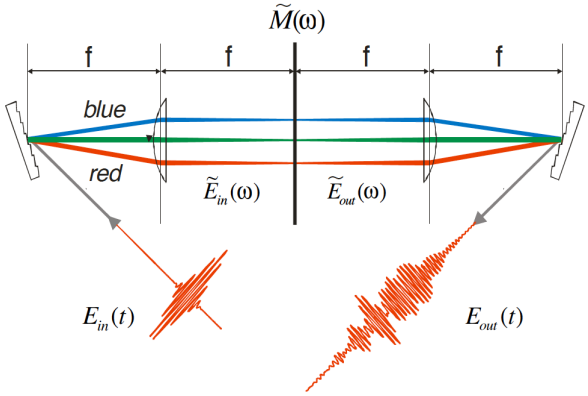

Figure 1: Basic layout for Fourier transform femtosecond pulse shaping (from [13]).

Recent discussion on ultrafast optical pulse shaping methods is centered mainly in waveform synthesis achieved by spatial masking of the spatially dispersed optical frequency spectrum, particularly in the use of Space Light Modulators (SLMs) which allow for reprogrammable waveform generation under computer control. The most commonly used SLMs are the Liquid Crystal SLMs (LC-SLMs) and the Acousto-optic Modulators (AOMs).

LC-SLMs are reported to contain up to 10^6 pixels [14], which allow for an immensely large number of different spectrally phase modulated pulses to be produced. As for AOMs, the use of a 2.5 cm long TeO_2 crystal has resulted in a group delay range of 3 ps, 6.7 fs temporal resolution and 30% diffraction efficiency[15].

In general, pulse shapers based on LC-SLMs have low transmission losses, are suitable for high repetition rate mode-locked laser oscillators, do not impose additional chirp and have a low waveform update rate on the order of 10 Hz. Set ups based on AOMs have high transmission losses, they do impose additional chirp but they have a waveform update rate in the order of 100 kHz. Both are suitable for amplitude and phase modulation, while programmable polarization shaping has been demonstrated, so far, only with LC-SLMs [16–23]. Extensive reviews on this topic may be found in [10, 13, 24].

2.2. Volume Bragg Gratings

Volume Bragg Gratings (VBGs) are Bragg Gratings which are recorded inside transparent material, usually in the form of a cube or a parallelepiped [25].

Recent decades have presented us with numerous publications on theoretical and experimental studying of VBGs written in various phase photosensitive media and used in many different configurations. The most widely accepted basis for description of such gratings, and which is as well adopted for this work, is the Theory of Coupled Waves, developed by Kogelnik in 1969 [26]. According to it, the *Bragg condition* for VBGs turns into [27]:

$$2\Lambda = \frac{\lambda_0}{n_{av}|cos(\theta_m^*)|} \tag{1}$$

where, here, λ_0 still denotes free-space wavelenght, Λ the grating period, n_{av} is the average refractive index of the medium and θ_m^* is the incident Bragg angle in a medium.

As for the sensitive media, one of the most promising materials for VBGs, and the one used is this work, is a phothermorefractive (PTR) glass which is a silicate glass doped with silver, cerium and fluorine [28]. PTR glass presented itself as a successful solution when used for high-efficiency holographic elements in high-power laser systems [29, 30]. Besides that, PTR glass possesses all the advantages of optical glass, such as thermal stability, high laser damage threshold, and wide transparency range. [31]

As the name suggests, CVBGs are non-uniform volume Bragg gratings, which basic chacteristics are identical to the previous described gratings, but having its spatial period (Λ) gradually changing along the whole volume.

Figure 2 (b) shows recording geometry for this gratings, being the case of uniform gratings repeated to provide means for comparison. If uniform volume gratings are produced by recording interference patterns of two collimated beams in photosensitive materials, CVBGs are obtained by recording this same sequences using a divergent beam and a convergent one. In the figure one may observe that the period changes in Z-direction, which is perpendicular to the bisector of the beams. Using two

identical beams, a linearly chirped grating is obtained.

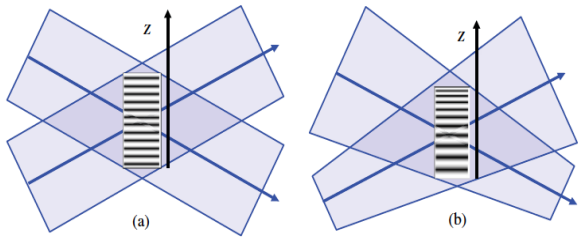

Figure 2: Recording geometry for uniform gratings by interference of collimated beams (a) and for chirped gratings by interference of a convergent and a divergent beams (b). Arrows show the direction of the recording beam propagation. Z is the axis collinear to the grating vector (from [12]).

As mentioned above, this work made use of such a grating in a Bragg mirror configuration, where period variation is directed along beam propagation direction. Figure 3 (c) shows such a configuration. From this configuration follows that the same wavelength may experience different distances, depending from which side we illuminate the grating. The side with larger grating period is called the *red end*, where larger wavelengths are to experience lesser distances, according to Bragg condition. The opposite end of the CVBG is called the *blue end*.

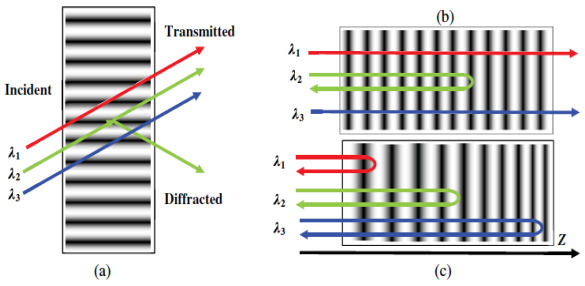

Figure 3: Schematics of beam diffraction by volume Bragg gratings. (a) Transmitting grating, (b) uniform reflecting grating (Bragg mirror), and (c) chirped reflecting grating, $\lambda_1 > \lambda_2 > \lambda_3$. Spatial modulation is not in scale: the typical period for a Bragg mirror at 1 μm is about 0.3 μm (from [12]).

It easily inferred that such a grating can be considered, locally, as Reflecting Bragg Grating, and as set of Bragg mirrors throughout its volume.

The Spectral Chirp Rate is a parameter that translates the amount of spectrum reflected when it travels a certain amount of space in the grating, and is defined as:

$$SCR = \frac{d\lambda}{dz}. \tag{2}$$

Taking into consideration the Bragg condition (1), and considering it for a general wavelength to be reflected on the grating, one may rewrite (2) as:

$$SCR = \frac{d\lambda}{dz} = 2n_{av}|cos(\theta_m^*)|\frac{d\Lambda}{dz} \tag{3}$$

where one may see, as expected, that the reflection spectrum of a CVBG depends on the chirp rate of the grating period itself, $d\Lambda/dz$.

Integrating (3), one obtains the expression for the total bandwidth of the grating:

$$\Delta\lambda = SCR \times t. \tag{4}$$

Finally, as one can see from fig. 3 (c), different wavelengths are going to experience different path sizes inside the grating. This will result in a delay between different spectral components. The total delay time (the maximum stretching) t_s between the spectral components corresponding to the front and back ends of a CBVG is determined by:

$$t_s = \frac{2n_{av}t}{c}. \tag{5}$$

The contents of this section are discussed in [12] and some of these concepts are presented with high detail in [32].

Spatial chirp is a very common spatio-temporal distortion in ultrafast optics, being frequently introduced by many routine operations in laser laboratories. It is said that a beam has spatial chirp whenever its different spectral components are separated in space, transversely to the propagation direction. The accuracy of pulse shaping depends greatly on the degree of spatial chirp at the focal plane. Refer to [33–35] for extensive studies on the subjected.

Spatial chirp in a CVBG is depicted in figure 4, where we have a top view of the grating.

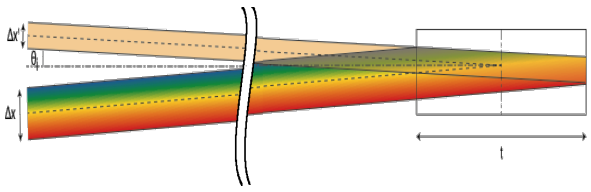

Figure 4: CVBG's top view depicting transversal chirp.

Figure 4 illustrate the mechanism by which one obtains spacial chirp in these gratings: pulses entering the grating with θ_i are to be diffracted and reflected back with angle θ_d. However, different wavelengths are reflected for different values of Z (or, alternatively, for different values of Λ). Thus, experiencing different distances in the grating, these componentes are also experiencing spacial separation.

For detailed information on spatial chirp one may refer to [36].

3. Numerical Model

This section's work is a simplified version of the one developed in [37]. It consists in considering CVBGs as set of smaller reflective Bragg gratings, each of which with different grating period Λ_n, and thickness $t_n = t/N$, where t is the overall thickness of the CVBG, while N is the number of segments one chooses to divide the grating into.

Consider figure 5, which represents a simplified schematic of a CVBG with N=4. The model shows equally spaced RVBGs reflecting parts of beam remaining from previously reflections.

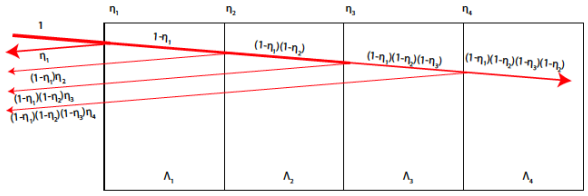

Figure 5: CVBG divided in 4 segments. The figure shows the amount of the initial beam that is diffracted by each of the individual reflecting gratings.

Considering the initial beam intensity to be normalized, from the analysis of the figure one may infer the following relation:

$$\eta(\lambda) = \eta_1(\lambda)+...+(1-\eta_3(\lambda)(1-\eta_2(\lambda))(1-\eta_1(\lambda))\eta_4(\lambda) \tag{6}$$

Where η is given by the following relations:

$$\Phi = -\frac{2\pi n_{av} t\delta n}{\lambda_0^2 f} \tag{7}$$

$$\xi(\Delta\lambda) = -\frac{\pi f t \Delta\lambda}{\lambda_0} \tag{8}$$

It results a diffraction efficiency, $\eta(\Delta\lambda)$, written:

$$\frac{sin^2\sqrt{\left(\frac{\pi f t\Delta\lambda}{\lambda_0}\right)^2 - \left(\frac{2\pi n_{av} t\delta n}{\lambda_0^2 f}\right)^2}}{\left(\frac{\lambda_0 f^2 \Delta\lambda}{2n_{av}\delta n}\right)^2 - cos^2\sqrt{\left(\frac{\pi f t\Delta\lambda}{\lambda_0}\right)^2 - \left(\frac{2\pi n_{av} t\delta n}{\lambda_0^2 f}\right)^2}} \tag{9}$$

where the parameters are defined as: the average refractive index of the medium n_{av} at free-space wavelength λ_0; an amplitude of refractive index modulation δn; the grating thickness t; the period Λ, or the correspondent spatial frequency $f = I/\Lambda$; and finally the inclination angle φ, between the normal to the front surface $\mathbf{N}_f$ and grating vector $\mathbf{K}_G$, which in turn is directed towards a medium perpendicular to the planes of a constant refractive index, having the module $|\mathbf{K}_G| = 2\pi i f$.

The generalization of such a relation for a general CVBG divided in N segments is straightforward. For simplicity's sake, lets first introduce the general function $h_n(\lambda)$, representing each term of the sum:

$$h_m(\lambda) = \eta_m(\lambda) \times \prod_{j=1}^{m-1}\Big(1-\eta_j(\lambda)\Big) \tag{10}$$

Finally, total diffraction efficiency comes written as:

$$\eta(\lambda) = \sum_{i=1}^{N} h_i(\lambda) = \sum_{i=1}^{N}\eta_i(\lambda) \times \prod_{j=1}^{i-1}\Big(1-\eta_j(\lambda)\Big). \tag{11}$$

Upon analysis of figure 6, one arrives to the following conclusions: With a non-zero diameter beam, the maximum number of segments which may contribute to a particular position x it's a function, as we can see, of beam diameter, as well as incident angle: the larger the beam, or the smaller the incident angle, more reflections from different segments are going to be present at a particular position in the mask plane.

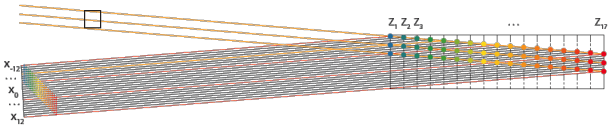

Figure 6: CVBG divided in 17 segments. More than one plane contributes for the same x coordinate.

one may infer that the maximum grating distance, from which one observer at x_0 may perceive contributions from the incident beam, comes:

$$\Delta z = \frac{D}{2sin\theta_i} \tag{12}$$

Taking into account the fact that each segment has thickness t/N, one may easily deduce the maximum number of segments that may contribute to a given position x in the mask plane:

$$S = Int\Big(\frac{\Delta z}{t/N}\Big) = Int\Big(\frac{N\Delta z}{t}\Big) \tag{13}$$

Obviously, the least number of segments contributing for one particular position is 1.

As show in figure 6, the segment discretization of the grating leads to a discretization of the x axis as well. Here, the number of segments can be calculated from the combinations of Z-segments' contributions present in each one of them, and it comes:

$$N_x = 3S - 2 \tag{14}$$

From this one may infer the total diameter of the reflected beam:

$$\Delta x' = \Delta x \frac{3S-2}{N} \tag{15}$$

where $\Delta x = 2tsin\theta$ is the total diameter of the reflected beam for a 0 diameter incident beam. Here, we have assumed that size of each interval in x axis is the same as in the previous case, and given by $\frac{\Delta x'}{3S-2} = \frac{\Delta x}{N}$.

Thus, the the total efficiency formula, for each x segment and for a given wavelength is writen:

$$H(n,\lambda) = \sum_{i=N/2+n-S/2}^{i=N/2+n+S/2} h_i(\lambda) \tag{16}$$

where:

- $n = \left[-\frac{N_x}{2}, ...0, ...\frac{N_x}{2} \right]$
- $x \in \left[n\frac{\Delta x}{N}, (n+1)\frac{\Delta x}{N} \right]$
- the grating segments contributing for a given segment in x are the limits of the sum, given by $i = \left[\frac{N}{2} + n - \frac{S}{2}, ...\frac{N}{2} + n, ...\frac{N}{2} + n + \frac{S}{2} \right]$

3.1. Verification and Validation

In [38] it is presented a study on the variation of refractive index modulation, δn, for RVBGs, according to (9). Both simulations, from the cited article and mine, are depicted in figure 7. From this analysis one is able to observe that a decrease in both refractive index modulation and grating thickness results in a decrease of diffraction efficiency. This was also easily anticipated given the role of these parameters in (7).

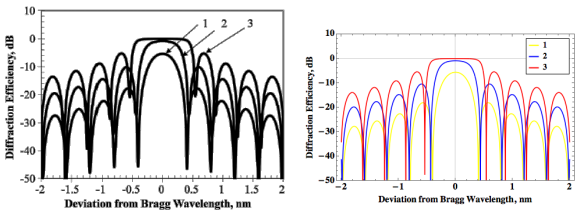

(a) Results from [38] (b) Achieved simulation

Figure 7: Dependence of diffraction efficiency of a RVBG on deviation from resonant wavelength λ_0 = 1985 nm, for monochromatic plane waves at normal incidence. Thickness 1 mm, average refractive index n_{av} = 1.4867. Refractive index modulation, ppm: 1= 200, 2= 500, 3 =1000.

Before using the developed model on my laboratory specifications, I will first test it on the results obtained in [12]. In it, the authors study diffraction efficiency response for different SCRs, eq. (3). Paper's results, along with the application of this work's model, are presented in fig. 8. It can be seen that all the plot is 8 (b) are overlapping each other, being the different colours indistinguishable. We may conclude that this model does not describe properly changes is the grating's chirp. This result should be expected, since the model itself consists in dividing the structure in equally spaced segments, which proves here to be insufficient in taking into account this chirp differences.

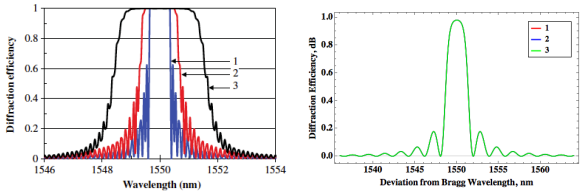

(a) Results from [12] (b) Achieved simulation

Figure 8: Modeled spectra of diffraction efficiency of CVBG with different spectral chirp rates (SCRs). Parameters of modeling: central wavelength λ_0 = 1550 nm, spatial refractive index modulation δn = 700 ppm, and thickness t = 5 mm, SCR dλ/dz, nm/cm: 1-0; 2-0.5; and 3-5, respectively.

In figure 9 (b) I show the modeling of the diffraction efficiency for the CVBG I've used in the experiments. In fig. 9 (a) it is shown the results obtained in [37], where the model used is a more complete version of one presented in this work. In both simulations one easily perceives that maximum efficiency doesn't reach 1. Besides that, a similiar behaviour is observed, having the grating a spectral bandwidth of operation of, approximately, 12 nm, which corresponds to fabric specifications.

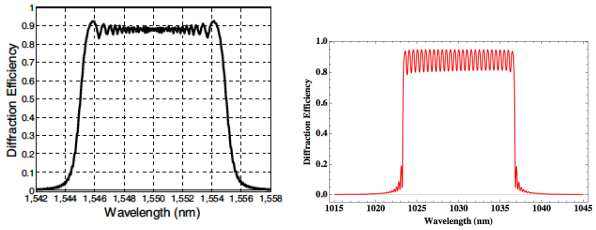

(a) Results from [37] (b) Achieved simulation

Figure 9: Diffraction efficiency of a CVBG, using partition methods. (a) grating parameters: Normal incidence, λ_0 = 1550 nm, t = 10 mm, N = 30, n_{av} = 1.5, δn = 800 ppm; (b) grating parameters: θ_i = 7.5°, λ_0 = 1030 nm, t = 33 mm, N = 30, n_{av} = 1.499, δn = 530 ppm.

Finally, spatial chirp simulation is shown in fig. 10. Hotter colours mean higher intensities, while the purple zone correspond to 0 intensity observed. It is possible to see that, for a given segment in x, one may find limited non-zero bandwidth, which

makes pulse shaping a difficult task. However, a linear relation between x and λ is also observed, which means for different segments in x one may also find a different set of wavelengths, allowing thus for a better pulse shaping control. These are expected spatial chirp properties, if we take into account the analysis developed before.

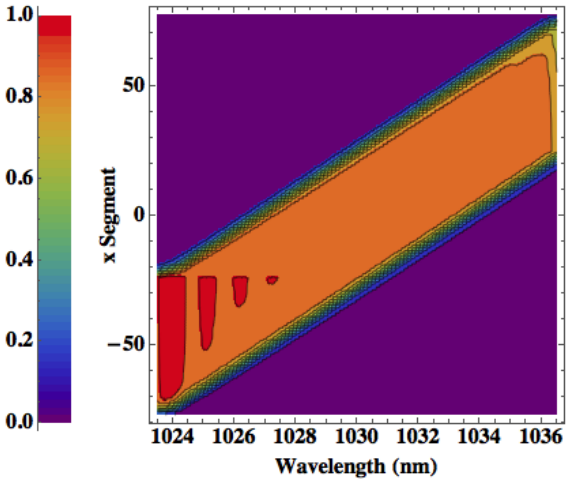

Figure 10: Spatial Chirp simualtion, where to hotter colours correspond higher intensities. Purple: 0 Intensity; Orange: Intensity = 0.9; Grating parameters: $\theta_i = 7.5°$, $\lambda_0 = 1030$ nm, t = 33 mm, N = 30, $n_{av} = 1.499$, $\delta n = 530$ ppm.

4. Experimental Measurements

Employed grating was purchased from Optigrate (optigrate.com).

4.1. Spectral Analysis for Transmitted and Reflected Beams

Comparison between simulated and real normalized reflected beam is shown in figure 11, for $\theta_i = 7.5°$. Reality shows us a more gaussian-like form, where two remarks should be pointed out: first, central wavelength for the first case (1030nm) is essentially the same as maximum point of the later (which was measured to be 1030.54 nm); second, FWHM for the measured beam is 10,9 nm, slightly less than spectral bandwidth of the simulated grating, estimated by Optigrade to be 13 nm. The overall reflected spectrum, however, is approximately 1 nm bigger.

4.2. Spatial Chirp

A 0.4 mm diameter fiber was connected to a spectrometer and to a mobile stage. Upon incident angle variation, the reflected spectrum would be scanned upon stage movement, in one fiber diameter steps.

From figure 12 one may draw the inference about the areas where pulse shaping is possible and easier. In particular, for $\theta_i = 7.5°$, 5.2 mm of beam is suitable for pulse shaping, having a rate of change of 1.6 nm per millimetre.

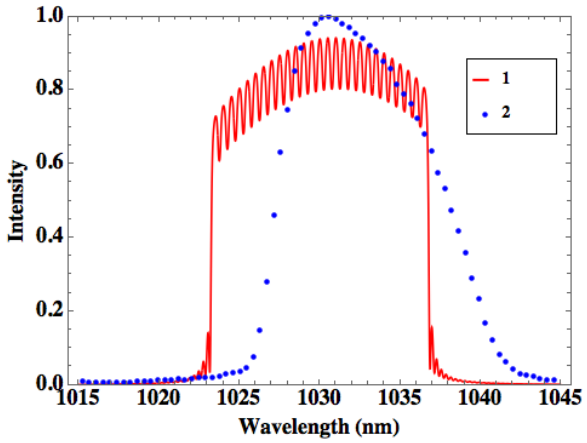

Figure 11: Comparison between experimental and simulated results. 1 - Diffraction efficiency of a CVBG, using partition methods. Grating parameters: $\theta_i = 7.5°$, $\lambda_0 = 1030$ nm, t = 33 mm, N = 30, $n_{av} = 1.499$, $\delta n = 530$ ppm. (b); 2 - Reflected Beam at $\theta_i = 7.5°$

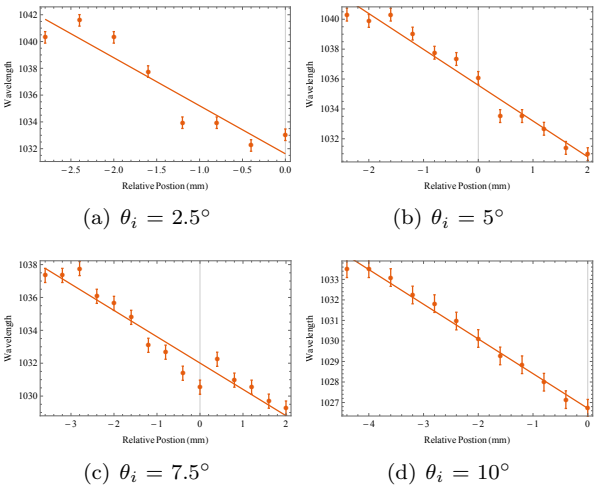

(a) $\theta_i = 2.5°$ (b) $\theta_i = 5°$

(c) $\theta_i = 7.5°$ (d) $\theta_i = 10°$

Figure 12: Horizontal chirp analysis for reflected beams, for several incident angles. Relation between central wavelength and its relative position in the beam.

5. Conclusions

No analysis was performed regarding incident beam diameter, in spite of its importance on the developed numerical model, due to the complexity of changing this parameter and the unavailability of a laboratory time slot. On the other hand, since the laboratory only possessed one CVBG, it was impossible to study the impact on pulse shaping characteristics of important grating parameters such as refractive index modulation or grating thickness. Fu-

ture work should be done to account the influence of these parameters on reflected beams.

One should also note that although numerical work presented itself important, insightful and sufficient, some improvements may still be implemented. Better models would allow for better simulations, facilitating comprehension of these materials, accelerating laboratory work, and enlightening the way for future tests, work and applications. Probably one of the most important effects inside a CVBG is the interference occurring between the several different beams. For the sake of simplicity and time, I've chosen to neglect such an effect, but future endeavours should try to take it into account.

Finally, the major achievement of this work was arriving to the conclusion that Chirp Volume Bragg Gratings are suitable materials for Pulse Shaping realization. It served also to define its main constraints and requirements for a proper accomplishment of such goal. We now know that bigger incident angles yield better results, but at the moment it is more complicated to say what influence would parameters such as granting thickness or the beam diameter have on reflected beams. Future efforts should include the realization of an actual pulse shaping system using CVBG and optimized already for all the key parameters.

Acknowledgements
This work could not be accomplished without the valuable support and experience of Gonçalo Nuno Marmelo Foito Figueira. The author is also especially thankful to Hugo Pires for the help in the experiment, and to all Group of Lasers and Plasmas, for the prompt availability to help whenever necessary, as well as for providing excellent work environment.

References

[1] Debabrata Goswami. Optical pulse shaping approaches to coherent control. *Physics Reports*, 374(6):385–481, 2003.

[2] Kenji Ohmori. Wave-packet and coherent control dynamics. *Annual review of physical chemistry*, 60:487–511, 2009.

[3] Marcos Dantus and Vadim V Lozovoy. Experimental coherent laser control of physicochemical processes. *Chemical reviews*, 104(4):1813–1860, 2004.

[4] Sang-Hee Shim and Martin T Zanni. How to turn your pump–probe instrument into a multidimensional spectrometer: 2d ir and vis spectroscopies via pulse shaping. *Physical Chemistry Chemical Physics*, 11(5):748–761, 2009.

[5] Yaron Silberberg. Quantum coherent control for nonlinear spectroscopy and microscopy. *Annual review of physical chemistry*, 60:277–292, 2009.

[6] Anatoly Efimov, Mark D Moores, B Mei, JL Krause, CW Siders, and DH Reitze. Minimization of dispersion in an ultrafast chirped pulse amplifier using adaptive learning. *Applied Physics B*, 70(1):S133–S141, 2000.

[7] Sébastien Weber, Béatrice Chatel, and Bertrand Girard. Factoring numbers with interfering random waves. *EPL (Europhysics Letters)*, 83(3):34008, 2008.

[8] Damien Bigourd, Béatrice Chatel, Wolfgang P Schleich, and Bertrand Girard. Factorization of numbers with the temporal talbot effect: optical implementation by a sequence of shaped ultrashort pulses. *Physical review letters*, 100(3):030202, 2008.

[9] HP Sardesai, CC Chang, and AM Weiner. A femtosecond code-division multiple-access communication system test bed. *Lightwave Technology, Journal of*, 16(11):1953–1964, 1998.

[10] Andrew M Weiner. Ultrafast optical pulse shaping: A tutorial review. *Optics Communications*, 284(15):3669–3692, 2011.

[11] Andrew M Weiner. Femtosecond pulse shaping using spatial light modulators. *Review of scientific instruments*, 71(5):1929–1960, 2000.

[12] Leonid Glebov, Vadim Smirnov, Eugeniu Rotari, Ion Cohanoschi, Larissa Glebova, Oleg Smolski, Julien Lumeau, Christopher Lantigua, and Alexei Glebov. Volume-chirped bragg gratings: monolithic components for stretching and compression of ultrashort laser pulses. *Optical Engineering*, 53(5):051514–051514, 2014.

[13] Matthias Wollenhaupt, Andreas Assion, and Thomas Baumert. Femtosecond laser pulses: linear properties, manipulation, generation and measurement. In *Springer Handbook of Lasers and Optics*, pages 937–983. Springer, 2007.

[14] Eugene Frumker and Yaron Silberberg. Femtosecond pulse shaping using a two-dimensional liquid-crystal spatial light modulator. *Optics letters*, 32(11):1384–1386, 2007.

[15] Frederic Verluise, Vincent Laude, Z Cheng, Ch Spielmann, and Pierre Tournois. Amplitude and phase control of ultrashort pulses by

use of an acousto-optic programmable dispersive filter: pulse compression and shaping. *Optics letters*, 25(8):575–577, 2000.

[16] Takashi Tanigawa, Yu Sakakibara, Shaobo Fang, Taro Sekikawa, and Mikio Yamashita. Spatial light modulator of 648 pixels with liquid crystal transparent from ultraviolet to near-infrared and its chirp compensation application. *Optics letters*, 34(11):1696–1698, 2009.

[17] D Zeidler, T Hornung, D Proch, and M Motzkus. Adaptive compression of tunable pulses from a non-collinear-type opa to below 16 fs by feedback-controlled pulse shaping. *Applied Physics B*, 70(1):S125–S131, 2000.

[18] Antoine Monmayrant and Béatrice Chatel. New phase and amplitude high resolution pulse shaper. *Review of Scientific Instruments*, 75:2668–2671, 2004.

[19] Brett J Pearson and Thomas C Weinacht. Shaped ultrafast laser pulses in the deep ultraviolet. *optics express*, 15(7):4385–4388, 2007.

[20] M Roth, M Mehendale, A Bartelt, and H Rabitz. Acousto-optical shaping of ultraviolet femtosecond pulses. *Applied Physics B*, 80(4-5):441–444, 2005.

[21] Howe-Siang Tan, Warren S Warren, and Elmar Schreiber. Generation and amplification of ultrashort shaped pulses in the visible by a two-stage noncollinear optical parametric process. *Optics letters*, 26(22):1812–1814, 2001.

[22] MA Dugan, JX Tull, and WS Warren. High-resolution acousto-optic shaping of unamplified and amplified femtosecond laser pulses. *JOSA B*, 14(9):2348–2358, 1997.

[23] Sang-Hee Shim, David B Strasfeld, Eric C Fulmer, and Martin T Zanni. Femtosecond pulse shaping directly in the mid-ir using acousto-optic modulation. *Optics letters*, 31(6):838–840, 2006.

[24] Antoine Monmayrant, Sébastien Weber, and Béatrice Chatel. A newcomer's guide to ultrashort pulse shaping and characterization. *Journal of Physics B: Atomic, Molecular and Optical Physics*, 43(10):103001, 2010.

[25] R. Paschotta. article on 'volume bragg gratings' in the encyclopedia of laser physics and technology. Wiley-VCH, October 2008. ISBN 978-3-527-40828-3.

[26] Herwig Kogelnik. Coupled wave theory for thick hologram gratings. *Bell System Technical Journal*, 48(9):2909–2947, 1969.

[27] Igor V Ciapurin, Leonid B Glebov, and Vadim I Smirnov. Modeling of phase volume diffractive gratings, part 1: transmitting sinusoidal uniform gratings. *Optical Engineering*, 45(1):015802–015802, 2006.

[28] Oleg M Efimov, Leonid B Glebov, Vadim I Smirnov, and Larissa Glebova. Proposed for the volume diffractive element (bragg grating) fabrication in photosensitive silicate glasses doped with silver, cerium, fluorine, and bromine. the process employs a photo-thermo-refractive (ptr) glass of high purity exposed uv, July 1 2003. US Patent 6,586,141.

[29] Leonid B Glebov, Vadim I Smirnov, C Martin Stickley, and Igor V Ciapurin. New approach to robust optics for hel systems. In *AeroSense 2002*, pages 101–109. International Society for Optics and Photonics, 2002.

[30] OM Efimov, LB Glebov, and VI SMIRNOV. High efficiency volume diffractive elements in photo-thermo-refractive glass: Us, 6673497.

[31] Leo A Siiman, Julien Lumeau, Lionel Canioni, and Leonid B Glebov. Ultrashort laser pulse diffraction by transmitting volume bragg gratings in photo-thermo-refractive glass. *Optics letters*, 34(17):2572–2574, 2009.

[32] Sergiy Kaim, Sergiy Mokhov, Boris Y Zeldovich, and Leonid B Glebov. Stretching and compressing of short laser pulses by chirped volume bragg gratings: analytic and numerical modeling. *Optical Engineering*, 53(5):051509–051509, 2014.

[33] JP Heritage, AM Weiner, and RN Thurston. Picosecond pulse shaping by spectral phase and amplitude manipulation. *Optics Letters*, 10(12):609–611, 1985.

[34] Marc M Wefers and Keith A Nelson. Space-time profiles of shaped ultrafast optical waveforms. *Quantum Electronics, IEEE Journal of*, 32(1):161–172, 1996.

[35] Marc M Wefers and Keith A Nelson. Analysis of programmable ultrashort waveform generation using liquid-crystal spatial light modulators. *JOSA B*, 12(7):1343–1362, 1995.

[36] Xun Gu, Selcuk Akturk, and Rick Trebino. Spatial chirp in ultrafast optics. *Optics Communications*, 242(4):599–604, 2004.

[37] Jiansheng Feng, Xiao Yuan, Xiang Zhang, Shang Wu, Kuaisheng Zou, and Guiju Zhang. Simulation of chirped volume bragg grating with a partition-integration method. PIERS.

[38] Igor V Ciapurin, Derrek R Drachenberg, Vadim I Smirnov, George B Venus, and Leonid B Glebov. Modeling of phase volume diffractive gratings, part 2: reflecting sinusoidal uniform gratings, bragg mirrors. *Optical Engineering*, 51(5):058001–1, 2012.